JOURNAL OF BACTERIOLOGY, Aug. 1990, p. 4510–4521
0021-9193/90/084510-12$02.00/0

Vol. 172, No. 8

Cloning and Characterization of *Kluyveromyces lactis SEC14*, a Gene Whose Product Stimulates Golgi Secretory Function in *Saccharomyces cerevisiae*

SOFIE R. SALAMA, ANN E. CLEVES, DAVID E. MALEHORN, ERIC A. WHITTERS, AND VYTAS A. BANKAITIS*

Department of Microbiology, University of Illinois at Urbana-Champaign, Urbana, Illinois 61801

Received 6 March 1990/Accepted 5 June 1990

The *Saccharomyces cerevisiae SEC14* gene encodes a cytosolic factor that is required for secretory protein movement from the Golgi complex. That some conservation of SEC14p function may exist was initially suggested by experiments that revealed immunoreactive polypeptides in cell extracts of the divergent yeasts *Kluyveromyces lactis* and *Schizosaccharomyces pombe*. We have cloned and characterized the *K. lactis SEC14* gene ($SEC14_{KL}$). Immunoprecipitation experiments indicated that $SEC14_{KL}$ encoded the *K. lactis* structural homolog of SEC14p. In agreement with those results, nucleotide sequence analysis of $SEC14_{KL}$ revealed a gene product of 301 residues (M_r, 34,615) and 77% identity to SEC14p. Moreover, a single ectopic copy of $SEC14_{KL}$ was sufficient to render *S. cerevisiae sec14-1*(Ts) mutants, or otherwise inviable *sec14-129::HIS3* mutant strains, completely proficient for secretory pathway function by the criteria of growth, invertase secretion, and kinetics of vacuolar protein localization. This efficient complementation of *sec14-129::HIS3* was observed to occur when the rates of $SEC14p_{KL}$ and SEC14p synthesis were reduced by a factor of 7 to 10 with respect to the wild-type rate of SEC14p synthesis. Taken together, these data provide evidence that the high level of structural conservation between SEC14p and $SEC14p_{KL}$ reflects a functional identity between these polypeptides as well. On the basis of the SEC14p and $SEC14p_{KL}$ primary sequence homology to the human retinaldehyde-binding protein, we suggest that the general function of these SEC14p species may be to regulate the delivery of a hydrophobic ligand to Golgi membranes so that biosynthetic secretory traffic can be supported.

We have been studying the *Saccharomyces cerevisiae SEC14* gene product, SEC14p. SEC14p was originally recognized as being involved in yeast Golgi function by the phenotypic, biochemical, and cytological behavior exhibited by *sec14*(Ts) mutants upon challenge with nonpermissive conditions (16). We have subsequently shown that SEC14p most likely plays a direct role in *S. cerevisiae* Golgi function, represents an activity that is essential for *S. cerevisiae* viability, and fractionates predominantly to the *S. cerevisiae* cytosol (1). On the basis of such data, we have proposed that SEC14p is a cytosolic factor that stimulates an essential Golgi secretory function. In keeping with the observation that cytosolic factors involved in stimulating eucaryotic Golgi secretory function have been functionally conserved (8, 12), we discovered that the divergent yeasts *Kluyveromyces lactis* and *Schizosaccharomyces pombe* exhibit polypeptides that are antigenically related to the *S. cerevisiae* SEC14p (1). It has become a matter of of interest, therefore, to determine the precise extent of the structural similarity implicit in this immunologic cross-reactivity and to determine whether this structural similarity is indicative of functional homology as well.

In this report, we present a detailed characterization of the *K. lactis SEC14* gene and of *S. cerevisiae sec14* mutants that express the *K. lactis SEC14* ($SEC14_{KL}$). Molecular analysis of $SEC14_{KL}$ revealed a 77% identity between SEC14p and $SEC14p_{KL}$ at the primary sequence level. Our data also indicated that $SEC14p_{KL}$ substituted for SEC14p in *sec14*(Ts) mutants and in mutants carrying haploid-lethal *sec14* disruption alleles. Furthermore, we observed that when these *S. cerevisiae sec14* disruption mutants exhibited intracellular concentrations of $SEC14p_{KL}$ that were reduced by a factor of 7 to 10 with respect to normal levels of SEC14p, wild-type growth and secretion were maintained. Similar results were obtained in experiments in which the threshold rate of SEC14p synthesis that supports efficient Golgi secretory function in *S. cerevisiae* was estimated. That is, we found that rates of SEC14p synthesis that were reduced by a factor of 7 to 10 relative to the wild-type rate had no measurable effect on secretory pathway function in *S. cerevisiae*.

Taken together, these data describe the structural and functional conservation between the SEC14p of *S. cerevisiae* and that of *K. lactis*. Some insight into the molecular basis for SEC14p function was provided by the significant homology of the SEC14p and $SEC14p_{KL}$ to the human retinaldehyde-binding protein. We suggest that the SEC14p is a carrier for a hydrophobic ligand whose participation is required to stimulate yeast Golgi secretory function.

MATERIALS AND METHODS

Genetic techniques. Yeast complex (YPD) and Wickerham minimal defined yeast media have been described elsewhere (22). Yeast transformations (14), gene disruption methods (17), and standard meiotic segregation analyses (22) have also been described elsewhere.

Escherichia coli MC1061 (1) and DH5 (13) were used for plasmid isolation and maintenance. Standard *E. coli* media were employed (23). Procedures for alkaline lysis purification of plasmid DNA and transformation of *E. coli* to

* Corresponding author.

ampicillin resistance with plasmid DNA have also been reported previously (23).

The *S. cerevisiae* haploid strains employed in this study included CTY1-1A [*MATa ura3-52 Δhis3-200 lys2-801*(Am) *sec14-1*(Ts)] and its isogenic *SEC14* derivative CTY182. Other isogenic derivatives included CTY235 (CTY1-1A *ura3-52*::pCTY28), CTY236 (CTY1-1A *ura3-52*::pKL6), CTY237 (CTY235 *sec14-129*::*HIS3*), and CTY238 (CTY236 *sec14-129*::*HIS3*). pCTY28 was obtained by inserting a 2.2-kilobase (kb) *Mlu*I-*Nru*I *S. cerevisiae* genomic DNA fragment that carried *SEC14* into the *Eco*RI-*Hin*dIII sites of YIp5 (3). pKL6 was constructed by inserting a 2.2-kb *Eco*RI-*Pvu*II fragment of the *K. lactis* genome that carried $SEC14_{KL}$ (see Fig. 1) and had been placed next to a polylinker *Sph*I site into the *Eco*RI-*Sph*I sites of YIp5. These plasmids were each recombined into the *ura3-52* locus of CTY1-1A by linearization at the unique *Stu*I site of the YIp5-borne *URA3* gene followed by transformation of CTY1-1A to Ura^+. These manipulations yielded strains CTY235 and CTY236, respectively. The CTY237 and CTY238 yeast strains were generated by recombining *sec14-129*::*HIS3* into CTY235 and CTY236, respectively. The *sec14-129*::*HIS3* allele was previously designated *SEC14*::*HIS3*, and details of its construction and introduction into yeast cells have been described elsewhere (1).

Reagents. The basic materials used throughout this work have been described elsewhere (1).

Cloning and characterization of $SEC14_{KL}$. Clones containing the $SEC14_{KL}$ gene were identified by their ability to complement the *S. cerevisiae sec14*(Ts) defect. The scheme employed to isolate such clones was exactly the same as the one used to obtain clones of the *S. cerevisiae SEC14* (1), with the exception that the transforming DNA was derived from the Salmeron and Johnston *K. lactis* genomic library propagated in the 2μm circle vector YEp24 (19). Physical mapping involved deletion and subcloning analyses coupled with phenotypic complementation. Subcloning experiments involved the introduction of defined restriction fragments from the complementing *K. lactis* DNA into the YEp24 derivative plasmid pSEY18 (9). Deletions within the insert were generated by standard means. Phenotypic complementation was determined by transformation of defined plasmid constructs into CTY1-1A by selection for Ura^+ at 30°C. Such transformants were subsequently tested for their ability to form single colonies at the restrictive temperature (37°C).

Immunoprecipitation of SEC14p and $SEC14p_{KL}$. In experiments in which SEC14p-cross-reactive materials were visualized, the appropriate yeast cells were grown to an early logarithmic growth stage (optical density at 600 nm [OD_{600}] = 0.5) in glucose (2%) minimal medium. The culture (cells with an OD_{600} of 0.5) was radiolabeled with 150 μCi of Trans-Label (>1,000 Ci/mmol; ICN Radiochemicals, Irvine, Calif.) for 20 min at 30°C. The incorporation of radiolabel was terminated by the addition of trichloroacetic acid (TCA) to a 5% final concentration, and the cells were subjected to disruption with glass beads. The preparation of clarified extracts, quantitative recovery of immune complexes, and evaluation of immunoprecipitates by sodium dodecyl sulfate-polyacrylamide gel electrophoresis (SDS-PAGE) and autoradiography have been described elsewhere (1, 21). The antibodies were used at a 1:500 dilution, and this dilution guaranteed antibody excess, as judged by the quantitative recovery of radiolabeled cognated antigen by this immunoprecipitation regimen.

DNA sequencing. Templates for DNA sequence analysis were generated by subcloning the appropriate restriction fragments into the pTZ phagemid vectors of Mead et al. (15). Phage M13K07 was employed as a helper for template synthesis. Nucleotide sequence analysis employed the chain termination method of Sanger et al. (20).

Invertase secretion. The appropriate yeast strains were grown to mid-logarithmic phase in YPD medium at 30°C with shaking. Cells were washed with 2 volumes of distilled water, resuspended in glucose (0.1%) YP medium, and incubated for 15 min at 30°C with shaking. The cultures were subsequently shifted to 37°C for 60 min, and total and extracellular invertase activities were determined (1). Invertase was assayed by the method of Goldstein and Lampen (11).

Immunoprecipitation of CPY and PrA. For the immunoprecipitation of carboxypeptidase Y (CPY) and proteinase A (PrA), yeast cells were grown to an early logarithmic growth stage (OD_{600} = 0.5) in glucose (2%) minimal medium at 30°C with shaking and were shifted to 37°C for 30 min. The cultures were radiolabeled (cells with an OD_{600} of 0.5) with 150 μCi of Trans-Label for 10 min, and chase was initiated by the addition of unlabeled methionine and cysteine to final concentrations of 1%. After 20 min, trichloroacetic acid was added to each culture (5% final concentration) and the precipitates were solubilized and subjected to immunoprecipitation, SDS-PAGE, and autoradiography as previously described (1).

Construction of specific deletions in *SEC14* upstream flanking regions. A series of eight DNA constructs that contained the intact structural gene and defined lengths of *SEC14* upstream genomic flanking sequence was generated. The *SEC14* gene, which extends from a genomic *Xba*I site at position −639 to a genomic *Bgl*II site at ca. +2000, was subcloned into the unique *Xba*I-*Bam*HI sites of the yeast centromere vector pSEYc68 (obtained from Scott Emr) to yield pCTY664. The −381 construct was represented as a 2.2-kb genomic *Mlu*I (at −381)-to-*Nru*I (at ca. +1800) fragment in plasmid pCTY28 (see above). Each of these two constructs was recovered as *Eco*RI-*Hin*dIII fragments and subcloned into the unique *Eco*RI-*Hin*dIII sites of YIp5. These plasmids were singly recombined into the *ura3-52* locus of CTYD43 (*MATa*/*MATα ura3-52*/*ura3-52 Δhis3-200*/*Δhis3-200 lys2-801*/*lys2-801 ADE2*/*ade2-101 TRP1*/*Δtrp1 SEC14*/*sec14-129*::*HIS3*) by linearization within the plasmid-borne *URA3* gene at the unique *Stu*I site, transformation, and selection of Ura^+ transformants.

Plasmid pRE30 was used to generate initial deletions into *SEC14* upstream flanking sequences. This plasmid was constructed by subcloning the 2.2-kb *Mlu*I-*Nru*I genomic *SEC14* fragment into the pUC9 vector in such a way that the *Mlu*I site directly abutted the *Eco*RI site. The inserted fragment was excised as an *Eco*RI-*Hin*dIII cartridge; the half-sites were rendered flush by a standard Klenow polymerase fill-in reaction and ligated into the *Sma*I site of pTZ18U (15) such that the 5′ end of the *SEC14* insert was proximal to the *Hin*dIII site of the pTZ18U multiple-cloning site. These manipulations generated pRE68. pRE68 was linearized by restriction with *Hin*dIII endonuclease and subjected to digestion by nuclease BAL 31 (Bethesda Research Laboratories, Gaithersburg, Md.). The digestion mixture consisted of the following ingredients: 100 μg of linearized pRE68 per milliliter in 20 mM Tris hydrochloride (pH 8.0)–12 mM $MgCl_2$–12 mM $CaCl_2$–200 mM NaCl–1 mM EDTA–0.01 U of enzyme per milliliter. Samples were removed at various time points and adjusted to 20 mM EGTA [ethylene glycol-bis (β-aminoethylether)-*N*,*N*,*N*′,*N*′-tetraacetic acid], and DNA

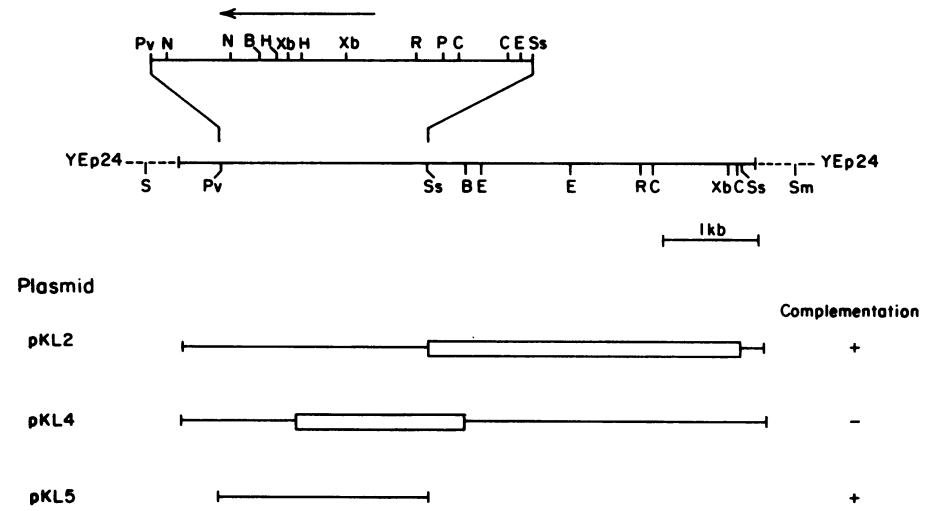

FIG. 1. Physical map of $SEC14_{KL}$. The 6.3-kb *K. lactis* genomic insert, represented in the *sec14-1*(Ts)-complementing plasmid pKL12 (see text), is shown. The $SEC14_{KL}$ coding region and direction of transcription are defined by the arrow. The lower part of the figure indicates the strategy by which $SEC14_{KL}$ was localized. Deletions internal to the insert (designated by open boxes) were generated between restriction sites uniquely represented in the insert, i.e., *Sst*I and *Bam*HI for pKL2 and pKL4, respectively. pKL5 identifies the 2.2-kb *Pvu*II-*Eco*RI minimal complementing fragment. The physical map of this 2.2-kb fragment is depicted in the offset enhancement. For restriction sites indicated in this enhancement but not in the genomic insert map, no information as to their arrangement in insert sequences outside of the minimal complementing fragment is available. Restriction site abbreviations: B, *Bam*HI; E, *Eco*RI; R, *Eco*RV; C, *Cla*I; H, *Hin*dIII; N, *Nco*I; P, *Pst*I; Pv, *Pvu*II; S, *Sal*I; Sm, *Sma*I; Ss, *Sst*I; Xb, *Xba*I.

was recovered by ethanol precipitation. The digestion products were ligated to commercially obtained *Sst*I linker oligonucleotides (Pharmacia, Piscataway, N.J) and used to transform *E. coli* KK2186 (1) to ampicillin resistance. The truncated gene products were recovered as *Sst*I-*Sst*I fragments and ligated into the *Sst*I site of pTZ18U to yield the −176 and −136 deletion constructs (pRE96 and pRE97, respectively). In both cases, the 5′ *SEC14* endpoint lay proximal to the vector *Eco*RI site. The precise nature of these deletion endpoints was determined by nucleotide sequencing.

A secondary round of deletion involved subjection of *Eco*RI-linearized pRE96 to nuclease BAL 31 digestion exactly as described above. Again digestion products were ligated to *Sst*I linkers and propagated in *E. coli* KK2186, and truncated constructs were recovered as *Sst*I-*Sst*I fragments. These were singly subcloned into the homologous sites of pTZ18R (15), and the resulting constructs were determined to exhibit deletion endpoints at positions −100, −72, −35, and −8 (yielding plasmids pRE483, pRE485, pRE487, and pRE489, respectively). Again, in all cases, the 5′ *SEC14* endpoints lay proximal to the vector *Eco*RI site. All six truncated *SEC14* constructs were recovered as *Eco*RI-*Hin*dIII fragments, subcloned into YIp5, and recombined into the *ura3-52* locus of strain CTYD43 as described above.

RESULTS

Isolation of $SEC14_{KL}$. We had previously demonstrated a conservation of *S. cerevisiae* SEC14p epitopes in the divergent yeasts *K. lactis* and *Schizosaccharomyces pombe* (1). To gain an initial assessment of the extent to which such an antigenic relatedness reflected a functional relatedness, we sought to obtain genomic clones of *K. lactis* genes that could complement or suppress the *S. cerevisiae sec14*(Ts) defect. If structural homology is representative of functional homology, the functional *SEC14* homolog from *K. lactis* should direct the expression in *S. cerevisiae* of the *K. lactis* polypeptide that exhibits immunological cross-reactivity with the *S. cerevisiae* SEC14p. Our efforts to isolate clones of such a functional homolog were facilitated by the recessive character of *sec14*(Ts) (1, 16) and by the fact that *K. lactis* genes can be expressed in *S. cerevisiae* (19, 24). As a result, we were able to identify the desired clones by direct selection.

Strain CTY1-1A [*ura3-52 sec14-1*(Ts)] was transformed with DNA isolated from a *K. lactis* genomic library maintained in the 2μm circle-based shuttle plasmid, YEp24. The desired transformants were selected on the basis of their expected Ura^+ Ts^+ phenotype (see Materials and Methods). From an estimated 11,000 potential Ura^+ transformants, we recovered 6 that exhibited a Ts^+ phenotype. Three of these Ura^+ Ts^+ transformants were analyzed for plasmid linkage of the Ts^+ character, and two independent methods were employed for these determinations. First, each candidate transformant was cured of its resident YEp24 derivative plasmid by 5-fluoroorotic acid challenge (2). In all cases, plasmid curing was accompanied by loss of the Ts^+ phenotype. Second, the resident plasmids were extracted from the candidate transformants, recovered in *E. coli*, purified, and retransformed into CTY1-1A via a Ura^+ selection. Again, in all cases, the Ura^+ transformants had acquired an unselected Ts^+ phenotype. Collectively, the data clearly demonstrated that these three candidate Ura^+ Ts^+ transformants harbored plasmids that bore *K. lactis* genes capable of complementing or suppressing the *S. cerevisiae sec14-1*(Ts) mutation.

A physical map of one such complementing plasmid insert (pKL12) is shown in Fig. 1. The pKL12 insert was only about 6.3 kb in length. Deletion analysis localized the complementing gene to the left of the 3.7-kb *Sst*I fragment that defined the right half of the pKL12 insert (Fig. 1). Additional subcloning experiments showed that a 2.2-kb *Eco*RI-*Pvu*II restriction fragment was necessary and sufficient for the *sec14-1*(Ts) complementing activity (pKL5; Fig. 1). Furthermore, the *Bam*HI site, the two *Hin*dIII sites, and

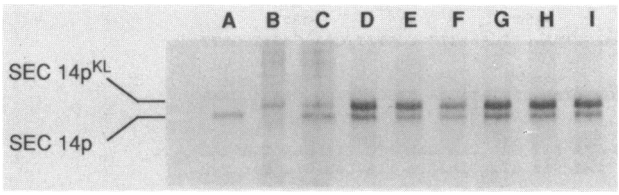

FIG. 2. The SEC14p-immunoreactive homolog of *K. lactis* also exhibits functional homology. Yeast strains were cultured in glucose (2%) minimal medium and allowed to incorporate radiolabel for 30 min at 30°C. Clarified extracts were recovered, and SEC14p-immunoreactive materials were displayed by SDS-PAGE and autoradiography. Lane A, *S. cerevisiae* CTY182 (*SEC14*); lane B, *K. lactis* MW98-8C; lane C, CTY182 mixed with MW98-8C. Precipitates from *S. cerevisiae* CTY1-1A [*sec14-1*(Ts)] carrying the *sec14-1*(Ts)-complementing YEp plasmids pKL1, pKL3, pKL7, pKL11, pKL12, and pKL13 are presented in lanes D through I, respectively. The positions of SEC14p and $SEC14p_{KL}$ are indicated at the left.

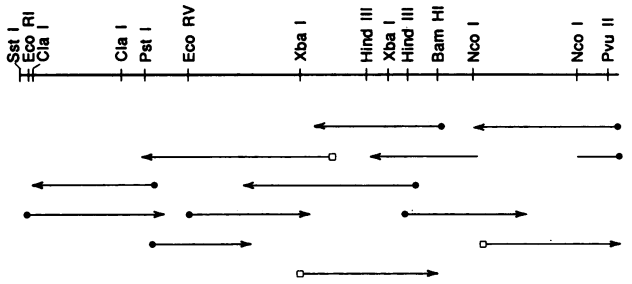

FIG. 3. Strategy for determination of $SEC14_{KL}$ sequence. The minimal complementing fragment is shown. The arrows indicate the extent and direction of individual sequencing runs employing either universal primer (Bethesda Research Laboratories) (●) or oligonucleotides corresponding to insert sequences (□).

the two *Xba*I sites that reside within this fragment were found to lie within the complementing gene. As we demonstrate below, this gene did not represent some dose-dependent suppressor of *sec14-1*(Ts) but was the true *SEC14* homolog of *K. lactis*. For simplicity, we shall henceforth refer to it as $SEC14_{KL}$. The direction of $SEC14_{KL}$ transcription was determined by generating strand-specific radiolabeled RNA probes by in vitro transcription, with the *Eco*RI-*Bam*HI restriction fragment derived from the *Eco*RI-*Pvu*II subclone as template, and hybridizing each probe to total *K. lactis* RNA fractions. A unique 1.3-kb RNA species was revealed by this approach, and it hybridized only to the probe that was transcribed in the *Bam*HI-to-*Eco*RI direction (data not shown). Thus, $SEC14_{KL}$ was transcribed in the *Eco*RI-to-*Bam*HI direction (Fig. 1).

$SEC14_{KL}$ encodes a structural homolog of *S. cerevisiae* SEC14p. The localization of $SEC14_{KL}$ to a minimal complementing fragment permitted a strict examination of whether $SEC14_{KL}$ encoded the SEC14p antigenic homolog previously observed in *K. lactis* extracts (1). *S. cerevisiae* CTY182, *K. lactis* MW98-8C, and *S. cerevisiae* CTY1-1A derivatives carrying appropriate $SEC14_{KL}$ plasmids were radiolabeled and analyzed for immunoreactive SEC14p species by quantitative immunoprecipitation (see Materials and Methods). As is apparent from the data presented in Fig. 2, treatment of CTY182 and MW98-8C extracts with SEC14p antiserum specifically revealed a unique polypeptide in each case. For CTY182, the 35-kilodalton SEC14p was recognized (Fig. 2, lane A), and a 38-kilodalton antigenic homolog was observed in the MW98-8C extracts (lane B). Mixing of CTY182 and MW98-8C extracts led to an autoradiography profile in which both species could be readily visualized (lane C). Analysis of extracts prepared from CTY1-1A carrying the minimal YEp24 ($SEC14_{KL}$) plasmid derived from pKL12 (designated pKL5) for SEC14p antigen revealed that both the *S. cerevisiae* and *K. lactis* forms of SEC14p were present (lane D). These data clearly demonstrate that $SEC14_{KL}$, originally represented by pKL12, encoded the *K. lactis* antigenic homology of *S. cerevisiae* SEC14p. These results show that the structural homology between SEC14p and $SEC14p_{KL}$ is indicative of some functional relatedness as well. We wish to emphasize that expression of $SEC14_{KL}$ in *S. cerevisiae*, while amplified by the multicopy nature of pKL12 (a YEp24 derivative), resulted in only an approximately twofold overrepresentation of $SEC14p_{KL}$ levels in the cell with respect to the intracellular levels of the homologous SEC14p (Fig. 2, lane D).

To investigate whether the other five potential $SEC14_{KL}$ recipients identified in the transformation of CTY1-1A to Ura^+ Ts^+ had indeed received this gene (see above) or had received some other functionally related gene whose product in high dosage could suppress *sec14-1*(Ts) defects, the SEC14p profiles of these strains were also determined. The data show that, in all cases, both SEC14p and $SEC14p_{KL}$ were represented (Fig. 2, lanes E to I). Thus, all of the *sec14-1*(Ts)-complementing genes of *K. lactis* origin that were analyzed yielded the same $SEC14_{KL}$.

$SEC14_{KL}$ nucleotide sequence. The apparent functional relatedness of SEC14p and $SEC14p_{KL}$ prompted us to compare their inferred primary sequences so as to determine the similarity between these polypeptides. This required elucidation of the $SEC14_{KL}$ nucleotide sequence. Localization of $SEC14_{KL}$ to a 2.2-kb *Eco*RI-*Pvu*II restriction fragment, in conjunction with the identification of restriction sites within the gene (Fig. 1), yielded a strategy by which the $SEC14_{KL}$ sequence was determined (Fig. 3). The *Eco*RI-*Pvu*II minimal complementing fragment consisted of 2,136 base pairs and exhibited a single, large open reading frame that was punctuated by tandem UAA and UAG termination codons. The nucleotide sequence of a 1,426-base-pair *Eco*RV-*Nco*I restriction fragment containing that entire open reading frame, along with the inferred primary sequence of its product, is given in Fig. 4. Clearly, this open reading frame represented $SEC14_{KL}$ for the following reasons. First, it spanned 301 continuous codons and exhibited the potential to encode a polypeptide with an M_r of 34,615. This predicted molecular mass was generally consistent with the mobility of $SEC14p_{KL}$ in denaturing gels. Second, it exhibited the expected polarity, as indicated by the direction of transcription experiments (see above). Third, it spanned the appropriate restriction sites that were shown to lie within $SEC14_{KL}$ (i.e., *Bam*HI, the two *Hin*dIII sites, and the two *Xba*I sites) (Fig. 4). We noted the absence of canonical splicing signals within the sequence. Since *S. cerevisiae* and *K. lactis* appear to employ the same highly conserved mRNA-splicing signals (6), we interpreted this to indicate that $SEC14_{KL}$ lacks introns. This is in marked contrast to the *S. cerevisiae SEC14*, which exhibits a single 156-nucleotide intron at the extreme 5′ end of its protein-coding region (1). The fact that the intronless $SEC14_{KL}$ was completely functional in *S. cerevisiae* suggests that the *SEC14* intron is a dispensable feature of that gene.

Alignment of the inferred SEC14p and $SEC14p_{KL}$ primary sequences revealed an extensive homology between these two polypeptides (Fig. 5). SEC14p and $SEC14p_{KL}$ exhibited

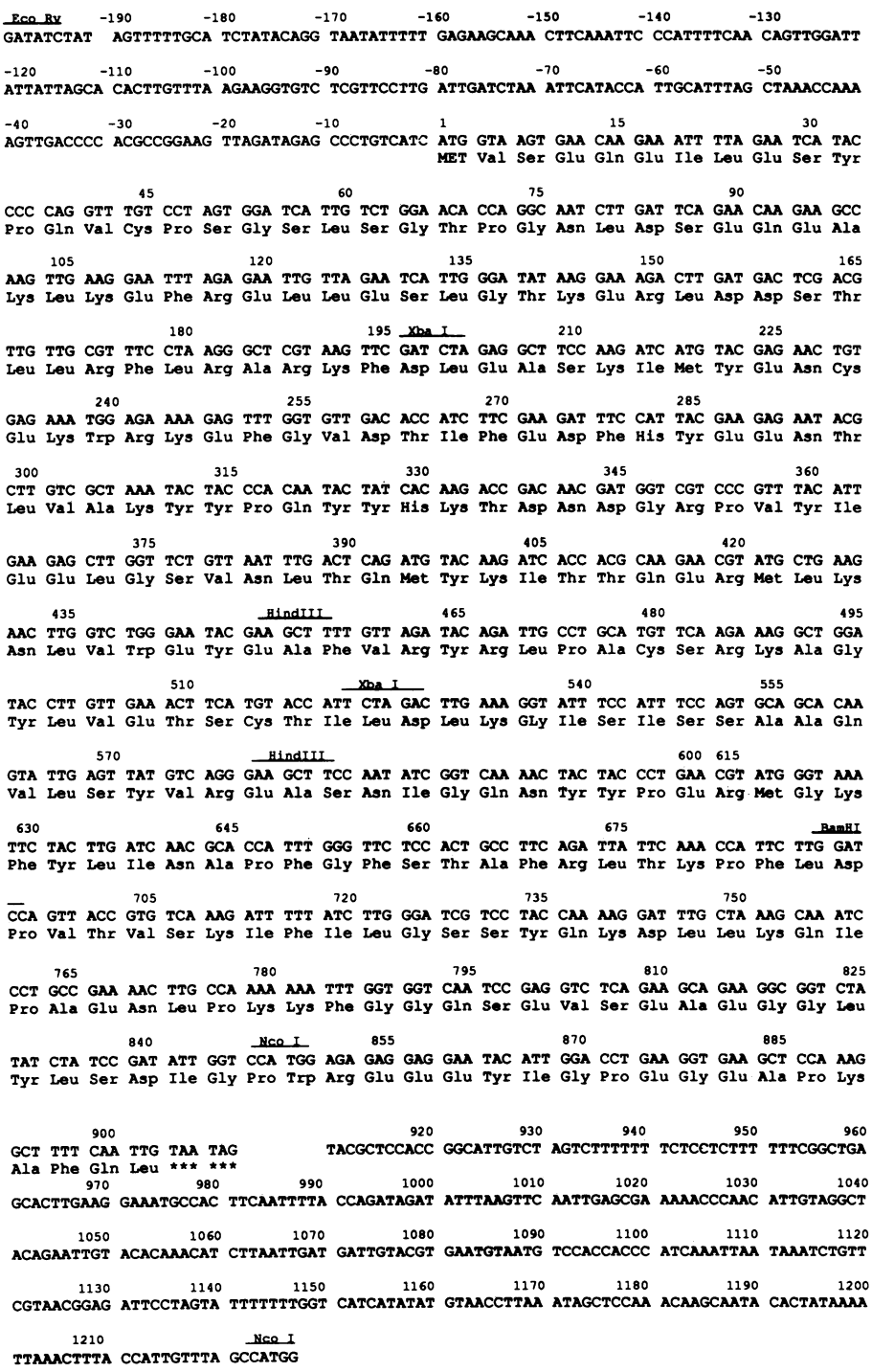

FIG. 4. Nucleotide sequence of *SEC14*$_{KL}$. The DNA sequence of the *SEC14*$_{KL}$ coding strand and the predicted primary sequence of its product are shown. Hallmark restriction sites that are referred to in the text are also shown.

a 77% identity at the primary sequence level, and this homology was evident throughout the protein sequence. Since SEC14p$_{KL}$ was three residues smaller than SEC14p, a two-residue gap and a one-residue gap needed to be introduced at the extreme amino and carboxy termini, respectively, of SEC14p$_{KL}$ to optimize the alignment (Fig. 5). The smaller size of SEC14p$_{KL}$ relative to SEC14p was not consistent with the relative mobilities of these polypeptides in SDS gels (Fig. 1), although we noted the slightly more acidic nature of SEC14p$_{KL}$ (pI = 4.9) as compared with SEC14p (pI = 5.3). It has been previously reported that a missense mutation resulting in the net addition of one more acidic amino acid to the maltose-binding protein primary sequence is sufficient to retard gel mobility to the same extent that was observed in the present study (4).

Given the extensive primary sequence homology shared by these two SEC14p species, we expected these two polypeptides to exhibit similar fractionation profiles. Strain

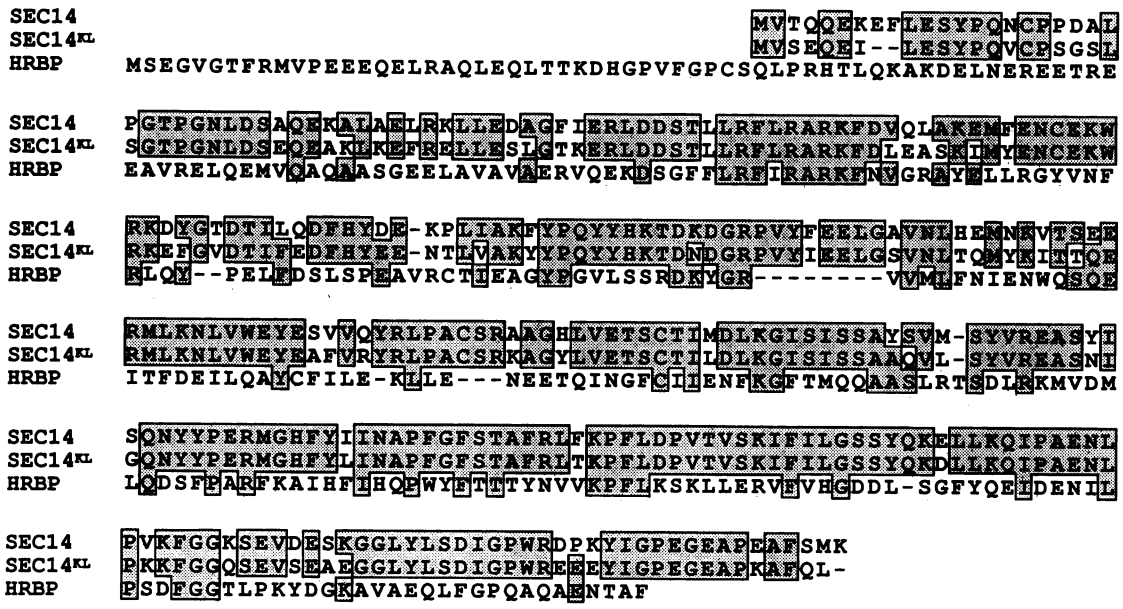

FIG. 5. Primary sequence comparison between SEC14p and SEC14p$_{KL}$. The primary sequences are given in single-letter code and aligned. Amino acid identities are boxed, while gaps are indicated by dashes (–). Sequence identities between these polypeptides and the human retinaldehyde-binding protein (HRBP) are also given (see text).

CTY182 carrying the YEp (*SEC14*$_{KL}$) plasmid pKL5 was subjected to our standard subcellular fractionation procedure, which has been previously described (1). The data indicated that the pKL5-driven SEC14p$_{KL}$ was distributed across the various analyzed subcellular fractions in exactly the same manner as the homologous SEC14p. That is, approximately 60% of the total SEC14p immunoreactive material was recovered from the 100,000 × *g* supernatant fraction, approximately 25% was recovered from the 100,000 × *g* pellet fraction, and approximately 10% was recovered from the 12,000 × *g* pellet fraction (not shown).

Although initial searches of the Protein Information Resource data base for primary sequences exhibiting homology to SEC14p were unproductive (1), subsequent comparisons of the SEC14p and SEC14p$_{KL}$ sequences to the Genentech data base revealed an interesting and significant homology. As shown in Fig. 5, the SEC14p exhibited a 25% identity over a stretch of 219 amino acids to the human retinaldehyde-binding protein primary sequence reported by Crabb et al. (5). This homology was considered significant, as the similarity between these polypeptides was some 10 standard deviations greater than that calculated for random sequences (data not shown). These SEC14p species did not exhibit immunological cross-reactivity with the human retinaldehyde-binding protein, however (unpublished data). Possible ramifications of this homology with regard to SEC14p function are given in Discussion.

SEC14p$_{KL}$ effectively substitutes for SEC14p in secretion of invertase. To determine the extent to which SEC14p and SEC14p$_{KL}$ are functionally related, we measured the efficiency of secretory pathway function in *S. cerevisiae sec14-1*(Ts) and *sec14* null mutants that bore an ectopic *SEC14*$_{KL}$ gene in single copy. The appropriate yeast strains for these experiments were constructed by integrating derivative YIp5 *SEC14* or *SEC14*$_{KL}$ plasmids into the *ura3-52* locus of CTY1-1A (see Materials and Methods). These manipulations generated strains CTY235 and CTY236, respectively. The nature of the expected integration events was confirmed by Southern analysis (results not shown) and meiotic segregation analysis. For the latter procedure, strains CTY235 and CTY236 were mated to CTY2-1C [MATa *ade2-101 sec14-1*(Ts)], the resultant diploids were sporulated, and four-spore asci were subjected to standard tetrad analysis. Data representative of an analysis of 20 tetrads from each cross revealed a 2 Ts$^+$:2 Ts$^-$ and 4 Ura$^+$:0 Ura$^-$ phenotypic pattern for all asci. The 2 Ts$^+$:2 Ts$^-$ segregation indicated that strains CTY235 and CTY236 had experienced single-site YIp5 (*SEC14*) and YIp5 (*SEC14*$_{KL}$) integration events, respectively. The inability of the tested strains to produce Ura$^-$ meiotic progeny indicated that the *ura3-52* locus was the site at which integration had occurred.

We observed that CTY235 and CTY236 grew at essentially wild-type rates at 37°C, which is normally a restrictive temperature for *sec14-1*(Ts) mutants. This result yielded two conclusions. First, the CTY235 data indicated that ectopic *SEC14* was functional when transposed to the *ura3-52* locus. Second, the behavior of CTY236 demonstrated that a single ectopic copy of *SEC14*$_{KL}$ was sufficient to compensate for the *sec14-1*(Ts) growth defect. The relative efficiency of this complementation with respect to secretion was determined by measuring the efficiency of invertase secretion to the cell surface in CTY235 and CTY236 at 37°C. As is evident from Table 1, the wild-type CTY182 exhibited all of its invertase activity at the cell surface. This was apparent because no latent invertase was detected in these cells. The isogenic *sec14-1*(Ts) strain (CTY1-1A) exhibited a markedly different invertase profile. Only some 39% of the total invertase was extracellular, and 61% was detected in a latent (i.e., intracellular) form. This distribution defined the uncompensated *sec14-1*(Ts) secretory block. Clearly, CTY235 was able to secrete invertase in a wild-type fashion, as the extracellular invertase measured for this strain accounted for the total invertase activity (Table 1). This was the expected result because CTY235 harbored an ectopic copy of the homologous *S. cerevisiae SEC14* in conjunction with the defective *sec14-1*(Ts) allele. That strain CTY236 also exhibited an

TABLE 1. Invertase secretion in *SEC14* and $SEC14_{KL}$ *S. cerevisiae*

Strain	Relevant genotype	Invertase activity[a]	
		Total	Extracellular (%) of total)
CTY18	*SEC14*	318	306 (>98)
CTY1-1A	*sec14-1*(Ts)	388	96 (25)
CYT235	*sec14-1*(Ts) *ura3-52*::*SEC14*	286	284 (>98)
CTY236	*sec14-1*(Ts) *ura3-52*::$SEC14_{KL}$	263	255 (97)
CTY237	*sec14-129*::*HIS3 ura3-52*::*SEC14*	260	258 (>98)
CTY238	*sec14-129*::*HIS3 ura3-52*::$SEC14_{KL}$	229	230 (>98)

[a] Data are representative of four independent experiments, and the given values represent averages of triplicate determinations for each sample. Invertase activity is expressed in nanomoles of glucose produced per minute at 30°C. For a description of these experiments, see Materials and Methods.

essentially wild-type pattern of secretion of invertase (>95% of the total invertase was extracellular [Table 1]) indicated a complete reversal of the *sec14-1*(Ts) secretory block by single-copy expression of an ectopic $SEC14_{KL}$.

We determined whether ectopic $SEC14_{KL}$ could, in single copy, complement the lethal disruption mutation *sec14-129*::*HIS3*. We found that this disruption allele could be introduced into the haploid strains CTY235 and CTY236 by linear transformation (see Materials and Methods), generating strains CTY237 and CTY238, respectively. Genomic Southern analysis (not shown) and immunoprecipitation of SEC14p crossreactive materials from these strains (see Fig. 7) confirmed that CTY237 and CTY238 were *sec14-129*::*HIS3* derivatives of CTY235 and CTY236, respectively. Both CTY237 and CTY238 exhibited wild-type growth at 25, 30, and 37°C. The fact that CTY238 showed wild-type behavior indicated that an ectopic $SEC14_{KL}$ gene, in single copy, was able to effectively complement what is essentially a *sec14* null allele. Quantitation of the efficiency of this complementation with respect to exocytosis was obtained from measurements of invertase secretion in this strain. The data presented in Table 1 demonstrate that both CTY237 and CTY238 exhibited wild-type distributions of secretory invertase activity. That is, the enzyme was localized exclusively to the cell surface.

$SEC14p_{KL}$ restores wild-type kinetics of vacuolar protein biogenesis to *sec14-1*(Ts) and *sec14-129*::*HIS3* mutants. As an independent measure of the ability of $SEC14p_{KL}$ to substitute for SEC14p in *S. cerevisiae*, we investigated the biogenesis of two proteinases of the vacuolar lumen, CPY and PrA, in *sec14-1*(Ts) and *sec14-129*::*HIS3* mutants expressing $SEC14p_{KL}$ from a single-copy gene. Both CPY and PrA exhibit distinct precursor forms (i.e., a core-glycosylated p1 form representative of material in transit through the endoplasmic reticulum and the Golgi apparatus and a p2 species that has acquired additional glycosyl modifications in the Golgi apparatus) and mature vacuolar forms that permit monitoring of the progress of radiolabeled proteinase through the secretory pathway to the vacuole (25, 27). In particular, as the proteolytic maturation that is associated with activation of these p2 zymogen forms is thought to occur in the vacuole (25, 27), the maturation event provides a convenient indicator for the arrival of these proteinases at the vacuole.

The appropriate yeast strains were incubated at 37°C, a restrictive temperature for *sec14-1*(Ts) mutants, for 30 min, pulse radiolabeled with ^{35}S-amino acids for 10 min, and

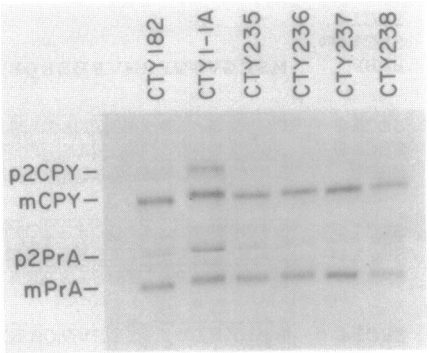

FIG. 6. $SEC14p_{KL}$ overcomes the *sec14-1*(Ts) defect in vacuolar protein biogenesis. *S. cerevisiae* strains were grown in glucose (2%) minimal medium at 30°C and shifted to 37°C for 30 min. Subsequently, cells were pulse radiolabeled for 10 min, and chase was initiated by addition of unlabeled methionine and cysteine to final concentrations of 1%. Chase was terminated with TCA (5%), and CPY and PrA cross-reactive materials were evaluated by immunoprecipitation, SDS-PAGE, and autoradiography. The yeast strains analyzed are given above the corresponding lanes, and precursor (p2) and mature (m) forms of CPY and PrA are indicated at the left.

subjected to a 20-min chase with excess unlabeled methionine and cysteine. Total cell protein was recovered by TCA precipitation, CPY and PrA cross-reactive materials were immunoprecipitated from clarified extracts, and the products were evaluated by SDS-PAGE and autoradiography (see Materials and Methods). Under these experimental conditions, the wild-type strain CTY182 exhibited essentially all of its radiolabeled CPY and PrA as the corresponding mature vacuolar species (Fig. 6). Only trace quantities of precursor forms were detected (<5% of total signal). That the isogenic *sec14-1*(Ts) mutant exhibited defects in CPY and PrA biogenesis at 37°C was indicated by the recovery of some 40% and 30% of the total radiolabeled material in the CPY and PrA precursor fractions, respectively. Detailed pulse-chase analyses indicated that the accumulated proCPY was almost exclusively in the p2 form, while the accumulated proPrA consisted of both p1 and p2 forms (data not shown). We also noted that, while the *sec14-1*(Ts) mutant was clearly defective for CPY and PrA biogenesis at the restrictive temperature, more than 60% of the labeled material had nevertheless matured by 20 min of chase and presumably represented material that had reached the vacuole (Fig. 6).

As expected, expression of the homologous SEC14p from an ectopic *SEC14* gene restored wild-type kinetics for biogenesis of CPY and PrA to the vacuole in *sec14-1*(Ts) mutants (CTY235) and the normally inviable *sec14-129*::*HIS3* mutants (CTY237) incubated at 37°C (Fig. 6). Expression of an ectopic $SEC14_{KL}$ elicited a similarly complete complementation of both the *sec14-1*(Ts) and *sec14-129*::*HIS3* lesions. The CPY and PrA autoradiographic profiles obtained for strains CTY236 [*sec14-1*(Ts) *ura3-52*::$SEC14_{KL}$] and CTY238 (*sec14-129*::*HIS3 ura3-52*::$SEC14_{KL}$) revealed almost exclusively the mature forms of these proteinases (Fig. 6). These profiles were indistinguishable from those obtained for the wild-type strain CTY182. We note that these pulse-chase conditions were designed to allow only wild-type cells to chase precursor forms of CPY and PrA to mature species (not shown). Consequently, this experimental method provided a sensitive measure of inefficiency in the biogenesis of CPY and PrA. The fact that single-copy expression of $SEC14_{KL}$

restored apparent wild-type rates of CPY and PrA biogenesis to *sec14-1*(Ts) and *sec14-129*::*HIS3* mutants was taken as further evidence of the functional relatedness of SEC14p and SEC14p$_{KL}$.

Intracellular levels of SEC14p synthesis in wild-type yeast cells exceed the amount required for normal secretory function. Our observation that single-copy expression of *SEC14*$_{KL}$ effected a complete restoration of viability and secretory pathway function to *sec14-129*::*HIS3* mutants was rather unexpected. The data had indicated that expression of multicopy *SEC14*$_{KL}$ in *S. cerevisiae* yielded intracellular levels of SEC14p$_{KL}$ that were only about two times greater than those observed for the homologous SEC14p expressed from its single chromosomal gene (Fig. 2; see above). Reduction of *SEC14*$_{KL}$ from a multicopy to a single-copy configuration in yeast cells would have been expected to result in a substantial reduction of SEC14p$_{KL}$ levels in such cells. The ability of an integrated *SEC14*$_{KL}$ to effectively complement recessive lethal *sec14* defects suggested that the wild-type yeast cells normally operate under conditions of SEC14p excess.

To test this possibility, we estimated the relative abundance of SEC14p and SEC14p$_{KL}$ in yeast strains in which the copy number of *SEC14*$_{KL}$ was varied. The appropriate yeast strains were radiolabeled at 30°C for 30 min, protein was precipitated with TCA, and SEC14p-immunoreactive species were quantitatively recovered and evaluated by SDS-PAGE and autoradiography. The results are shown in Fig. 7. The profile derived from yeast strain CTY1-1A(pKL12) revealed the two expected SEC14p-immunoreactive species: the *S. cerevisiae* SEC14p and the more slowly migrating SEC14p$_{KL}$ (Fig. 7). Note that, even though *SEC14*$_{KL}$ was in a multicopy configuration in this strain and *SEC14* was in a single-copy configuration, the SEC14p$_{KL}$ signal was increased only 1.5- to 2-fold over that of SEC14p. As expected, only the *S. cerevisiae* SEC14p was recovered from lysates prepared from CTY235, a strain that did not harbor any copies of *SEC14*$_{KL}$ (Fig. 7). The SEC14p profile obtained for strain CTY236 demonstrated that reduction of *SEC14*$_{KL}$ from a multicopy to a single-copy state markedly diminished the amount of radiolabeled SEC14p$_{KL}$ that was recovered from yeast cell extracts (Fig. 7). We observed that the *S. cerevisiae* SEC14p constituted the major immunoreactive species in such lysates. SEC14p$_{KL}$, while clearly detectable, was synthesized at only about 10 to 15% of the SEC14p level. The relative magnitude of this reduction was best appreciated by comparing the quantitative radiolabeled SEC14p profiles displayed in Fig. 7 [strains CTY1-1A(pKL12) and CTY236]. While the SEC14p signals in these lanes were very nearly equivalent, the SEC14p$_{KL}$ signal from the multicopy *SEC14*$_{KL}$ strain [CTY1-1A(pKL12)] was about 10 to 12 times stronger than that of the single-copy *SEC14*$_{KL}$ strain (CTY236).

Greatly reduced levels of SEC14p$_{KL}$ synthesis were also apparent in extracts prepared from strain CTY238, a *sec14-129*::*HIS3* mutant that harbors only a single ectopic copy of *SEC14*$_{KL}$. Examination of the immunoprecipitated materials recovered from CTY238 lysates revealed two SEC14p species (Fig. 7). By far the stronger signal was observed to reside in a species that migrated at an apparent molecular mass of about 16 to 18 kilodaltons and represented the nonfunctional *sec14-129*::*HIS3* gene product. Although this truncated SEC14p′ exhibited a total ^{35}S-amino acid content that was less than half that of the full-length SEC14p$_{KL}$, it nevertheless yielded a signal that was some three to four times more intense than the one detected for the

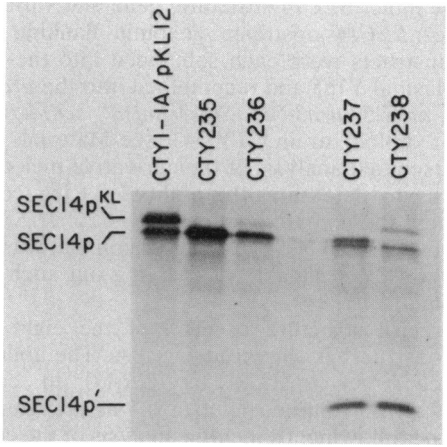

FIG. 7. Levels of SEC14p and SEC14p$_{KL}$ expression. *S. cerevisiae* CTY1-1A derivative strains were grown in glucose (2%) minimal yeast medium and allowed to incorporate radiolabel for 30 min at 30°C. Radiolabeling was terminated by the addition of TCA (5%). SEC14p-immunoreactive species were recovered from clarified extracts by immunoprecipitation, and precipitated materials were evaluated by SDS-PAGE and autoradiography. The strains from which the immunoprecipitates were derived are indicated above the autoradiogram. Relevant genotypes are given in Table 1 and Materials and Methods. The positions of SEC14p$_{KL}$, SEC14p, and the truncated *sec14-129*::*HIS3* gene product (SEC14p′) are indicated at left. The CTY237 and CTY238 lanes were approximately threefold overloaded with respect to the others so that SEC14p and SEC14p$_{KL}$ could be more readily visualized. The contaminating band migrating just below the position of SEC14p in these two lanes is not of SEC14p origin and became prominent, relative to the signal observed in the other lanes, because of this overloading.

SEC14p$_{KL}$. Taken together, these data suggested that single-copy expression of *SEC14*$_{KL}$ generated a level of SEC14p$_{KL}$ synthesis that was only approximately 10% of the normal level observed for the homologous SEC14p. That this reduced level was sufficient to restore wild-type secretory and growth properties to *sec14-1*(Ts) and *sec14-129*::*HIS3* mutants argued for an excess of SEC14p in the wild-type yeast cell. Initial support for this argument was also obtained from analysis of homologous SEC14p levels in strain CTY237, a *sec14-129*::*HIS3* mutant that harbors a single integrated copy of *SEC14* at the *ura3-52* locus and is isogenic to strain CTY238. Evaluation of the immunoprecipitates from this strain revealed the two anticipated SEC14p forms, the truncated *sec14-129*::*HIS3* gene product and the intact SEC14p (Fig. 7). The salient aspect of this pattern was that the full-length SEC14p elicited a signal that was essentially equivalent to that of the truncated gene product. Since SEC14p experienced a threefold overrepresentation of ^{35}S-amino acids with respect to the *sec14-129*::*HIS3* gene product, we estimated that expression of the ectopic *SEC14* was reduced by a factor of about three in CTY237 relative to wild-type levels.

Relationship of *SEC14* expression to the secretory capacity of *S. cerevisiae*. That reduction by a factor of approximately 10 in *SEC14*$_{KL}$ expression (relative to that of *SEC14*) was sufficient to endow the otherwise inviable *sec14-129*::*HIS3* mutant with wild-type secretory behavior raised the question of what the threshold level of SEC14p synthesis that supports efficient Golgi secretory function in *S. cerevisiae* is. To obtain an estimate of that minimal rate of *SEC14* expression, we generated a series of eight DNA constructs that con-

tained the intact *SEC14* structural gene and various defined lengths of *SEC14* upstream genomic flanking sequence. These constructs were each subcloned into the yeast integrating plasmid YIp5 and recombined into the *ura3-52* locus of the *ura3-52/ura3-52 Δhis3/Δhis3 sec14-1*(Ts)/*sec14-129*::*HIS3* diploid strain CTYD43 (see Materials and Methods). Subsequent analysis of the derivative meiotic progeny enabled us to determine the ability of each construct to complement the recessive-lethal *sec14-129*::*HIS3* allele and to measure the level of *SEC14* expression that was supported by each construct capable of carrying out such a complementation.

The precise structure of each of the eight integrated *SEC14* constructs is shown in Fig. 8A. The ability of each *SEC14* construct (marked by *URA3*) to complement *sec14-129*::*HIS3* (marked by *HIS3*) was recognized on the basis of the following: (i) meiotic analysis of the corresponding diploid strain yielding four-spore asci that exhibited a pattern better than the two viable progeny per ascus characteristic of asci derived from strain CTYD43, (ii) the detection of His^+ haploid progeny among the viable progeny derived from each of the deviant asci, and (iii) the finding that all such viable His^+ segregants also were Ura^+ (i.e., contained the integrated test construct). The results of such an analysis are also shown in Fig. 8A. The panel of *SEC14* constructs exhibited amounts of genomic flanking sequence that ranged from 639 nucleotides upstream of the *SEC14* initiator codon (designated as the +1 position) to only 8 nucleotides upstream. Single ectopic copies of *SEC14* with deletion endpoints at nucleotide −639, −381, −176, or −136 were able to complement *sec14-129*::*HIS3*, as judged by the criteria enumerated above. Integrated copies of *SEC14* with deletion endpoints at nucleotide −100, −72, −35, or −8 were not capable of supporting sufficient expression of *SEC14* to complement *sec14-129*::*HIS3* lethality. Thus, the *sec14-129*::*HIS3* haploid strain carrying the ectopic copy of *SEC14* with 136 nucleotides of upstream flanking sequence (CTY374) was a good candidate for a strain that was operating at or near the threshold level of *SEC14* expression. We note that all four ectopic *SEC14* constructs that complemented *sec14-129*::*HIS3* apparently did so completely. That is, the corresponding haploid strains (i.e., CTY366, CTY368, CTY372, and CTY374) exhibited wild-type growth rates at all temperatures, and no significant intracellular pools of secretory invertase were detected in these yeasts (as indicated by their secretion index) (Fig. 8A).

To measure the relative rates of SEC14p synthesis in the appropriate haploid strains, yeast cells were cultured in glucose minimal medium at 20°C and pulse radiolabeled with [^{35}S]methionine and [^{35}S]cysteine for 10 min. A chase period (20 min) was then initiated by addition of excess unlabeled methionine plus cysteine, and total protein was precipitated with TCA. Immunoreactive SEC14p and CPY material were recovered by quantitative immunoprecipitation and evaluated by SDS-PAGE and autoradiography. Since the SEC14p is a stable intracellular species (with a half-life on the order of hours; data not shown), the intensity of the signal observed in these experiments was directly related to the rate of SEC14p synthesis. The purpose of precipitating CPY antigen in these experiments was twofold. First, it served as a standard by which SEC14p levels could be normalized. Second, the CPY profile provided a direct measure of the efficiency of secretory pathway function in these various yeast strains. The data are presented in Fig. 8B.

Treatment of radiolabeled CTY366 extracts with CPY and SEC14p antisera precipitated four major radiolabeled species: p2CPY, mature CPY (mCPY), SEC14p, and the low-molecular-weight Sec14p′ species representative of the *sec14-129*::*HIS3* gene product. The level of SEC14p synthesis in this strain was equivalent to that observed in wild-type cells, as judged by the observation that the SEC14p signal exhibited approximate equivalence to the total CPY signal (p2CPY + mCPY). We have previously shown that SEC14p and CPY are synthesized at similar rates in wild-type *S. cerevisiae* (1). The ratio of p2CPY (40% of the total) to mCPY (60% of the total) was also representative of the rate of CPY biogenesis observed in wild-type *S. cerevisiae* under these labeling conditions (not shown).

Inspection of the CPY and SEC14p profiles obtained from extracts of strains CTY374 and CTY372 revealed that while the relative intensities of the p2CPY, mCPY, and *sec14-129*::*HIS3* gene product signals were essentially the same as those demonstrated for CTY366, the SEC14p signals observed for the first two strains were reduced with respect to the SEC14p signal seen for CTY366 (Fig. 8B). Densitometric measurements estimated that this reduction corresponded to decreases by factors of approximately 6 and 10 in the rate of SEC14p synthesis (relative to the wild-type rate) in strains CTY372 and CTY374, respectively. These reductions in the SEC14p synthesis rate were also manifested in the relative steady-state levels of SEC14p in these strains, as determined by quantitative immunoblotting of clarified extracts prepared from these yeast. Strains CTY372 and CTY374 exhibited reductions by factors of 5 and 7, respectively, in the steady-state levels of SEC14p relative to those exhibited by CTY366 and the wild-type strain (not shown). We also noted that the p2CPY-to-mCPY ratios for strains CTY374 and CTY372 were very similar to those observed for strain CTY366, indicating that the kinetics of CPY biogenesis in the first two strains were essentially wild type. On the basis of these data, we concluded that the minimal rate of SEC14p synthesis that supports efficient Golgi secretory function in *S. cerevisiae* was approximately 1/7 to 1/10 of that which is observed in wild-type yeast cells.

DISCUSSION

We had previously obtained evidence that suggested a conservation of aspects of SEC14p structure across wide phylogenetic boundaries. Such evidence was derived from experiments that revealed the presence of SEC14p-immunoreactive materials in cell extracts prepared from the budding yeast *K. lactis* and the fission yeast *Schizosaccharomyces pombe* (1). As a first step in assessing the functional ramifications of this immunological relatedness, we cloned and characterized the functional $SEC14_{KL}$ gene. In this report we show that $SEC14p_{KL}$ exhibited antigenic similarity, functional identity, and a high degree of primary sequence identity to *S. cerevisiae* SEC14p.

The demonstration of antigenic similarity between SEC14p and $SEC14p_{KL}$ was obtained from quantitative immunoprecipitation experiments in which both the SEC14p-immunoreactive *K. lactis* polypeptide and the homologous SEC14p were recovered from clarified extracts prepared from *S. cerevisiae* strains expressing $SEC14_{KL}$ (Fig. 2). The structural similarity implicit in this immunological cross-reactivity was readily evident in a comparison of the inferred primary structures of SEC14p and $SEC14p_{KL}$. These two polypeptides exhibited a 77% identity at the primary sequence level (Fig. 4). It is interesting that, in light of such similarity, $SEC14_{KL}$ exhibits no introns while the *S. cerevisiae SEC14* gene exhibits one.

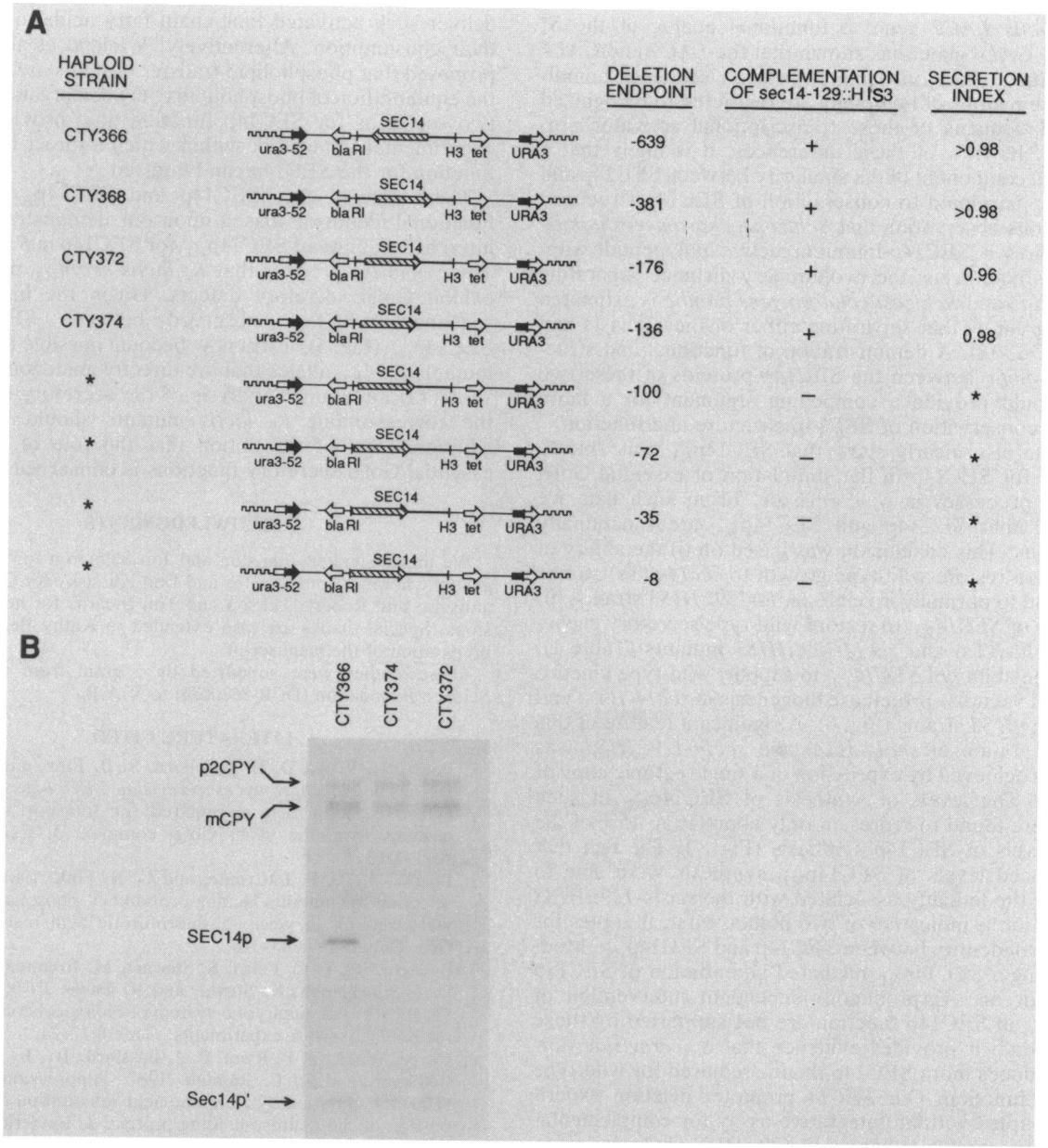

FIG. 8. Threshold rate of SEC14p synthesis. (A) *SEC14* upstream flanking sequence deletion constructs were recombined into the *ura3-52* locus of strain CTYD43 by linearization of these YIp5 derivatives at a *Stu*I site that resides within the vector-borne *URA3*. The precise products of the integration events, including the orientation of transcription of the relevant genes, are diagrammed. The positions of the *Eco*RI (RI) and *Hin*dIII (H3) sites that bound each *SEC14* construct are indicated, as are the corresponding upstream *SEC14* deletion endpoints. The ability of each of these ectopic *SEC14* constructs to complement the recessive-lethal *sec14-129*::*HIS3* lesion was determined by meiotic analysis (see text), and the results are given. Haploid progeny receiving a complementing construct and the *sec14-129*::*HIS3* allele were given strain designations as indicated, and their secretion indices were determined. The secretion index was determined by the following relationship: secretion index = secreted invertase/total invertase. The extracellular (i.e., secreted) and total invertase activities were determined exactly as described in Table 1, footnote *a*. The secretion index of wild-type yeast strains is typically >0.98 (Table 1). *, Not applicable. (B) Radiolabeled SEC14p and CPY profiles from strains CTY366, CTY374, and CTY372. Details of the experiment are provided in the text. The p2CPY, mCPY, SEC14p, and SEC14p' (i.e., the *sec14-129*::*HIS3* gene product) are identified by the arrows at the left.

At this point, it is still unclear to what extent the homology observed between SEC14p and SEC14p$_{KL}$ reflects a conservation of SEC14p structure as opposed to a moderate relatedness between *K. lactis* and *S. cerevisiae*. Comparative sequence analyses between the *GAL7* and *GAL10* gene products of these two organisms have revealed identities of 63% and 45%, respectively, at the primary sequence level (7). These findings might suggest that primary sequence identities at levels of approximately 60% will be commonly encountered in comparisons of *S. cerevisiae* gene products and their *K. lactis* counterparts. However, it should also be pointed out that these Leloir enzymes (i.e., the *GAL7*-encoded transferase and the *GAL10*-encoded epimerase) are conserved proteins in their own right. The corresponding *E. coli* enzymes exhibit primary sequence homologies of about 51% and 42% to those of *K. lactis* (7). Molecular analysis of

the *K. lactis LAC9* gene, a functional analog of the *S. cerevisiae GAL4* gene, has shown that the *LAC9* and *GAL4* gene products share only limited primary sequence homology. These regions of homology are restricted to recognized functional domains of these transcriptional activator proteins (19). In view of these differences, it is likely that a substantial component of the similarity between SEC14p and $SEC14p_{KL}$ is related to conservation of SEC14p structure. Our previous observation that *Schizosaccharomyces pombe* also displays a SEC14p-immunoreactive polypeptide supports this hypothesis; the evolutionary distance separating *S. cerevisiae* and *Schizosaccharomyces pombe* is estimated to be as great as that separating either of these yeasts and mammals (1, 18). A demonstration of functional and structural homology between the SEC14p proteins of these two yeasts would provide a compelling argument for a more universal conservation of SEC14p structure and function.

Our data also clearly show that $SEC14p_{KL}$ was able to substitute for SEC14p in the stimulation of essential Golgi secretory processes in *S. cerevisiae*. From such data we concluded that SEC14p and $SEC14p_{KL}$ are functionally homologous. This conclusion was based on (i) the ability of $SEC14_{KL}$ to restore wild-type growth to *sec14-1*(Ts) strains at 37°C and to normally inviable *sec14-129*::*HIS3* strains, (ii) the ability of $SEC14_{KL}$ to restore wild-type secretory capacity to *sec14-1*(Ts) and *sec14-129*::*HIS3* mutants (Table 1), and (iii) the ability of $SEC14_{KL}$ to support wild-type kinetics of lumenal vacuolar proteinase biogenesis in *sec14-1*(Ts) and *sec14-129*::*HIS3* strains (Fig. 6). A significant feature of this complementation of *sec14-1*(Ts) and *sec14-129*::*HIS3* was that it was achieved by expression of a single ectopic copy of $SEC14_{KL}$. The levels of synthesis of $SEC14p_{KL}$ in such strains were found to represent only about 10 to 15% of the normal levels of SEC14p synthesis (Fig. 7). The fact that such reduced levels of $SEC14p_{KL}$ synthesis were able to overcome the lethality associated with the *sec14-129*::*HIS3* null mutation is indicative of two points. First, it argues for a functional identity between SEC14p and $SEC14p_{KL}$. Models invoking a $SEC14p_{KL}$-mediated potentiation of SEC14p function or an overproduction-dependent intervention of $SEC14p_{KL}$ in SEC14p function are not supported by those data. Second, it provides evidence that *S. cerevisiae* normally produces more SEC14p than is required for wild-type secretory function. Our *SEC14* promoter deletion experiments, coupled with an integrative assay for complementation of the recessive-lethal *sec14-129*::*HIS3* allele, led us to estimate that the SEC14p is synthesized at rates that are about an order of magnitude greater than those minimally required for wild-type secretory pathway function in *S. cerevisiae* (Fig. 8).

Do these studies provide some insight into SEC14p and $SEC14p_{KL}$ function? An initial clue was provided by the significant homology of SEC14p and $SEC14p_{KL}$ to the human retinaldehyde-binding protein (Fig. 5). Since the biological function of this binding protein is to serve as a substrate carrier protein and stereoselective agent that delivers hydrophobic ligands (i.e., 11-*cis*-retinol and 11-*cis*-retinaldehyde) to the appropriate dehydrogenase in human retinal epithelium (5), we consider it likely that the SEC14p plays an analogous role, that is, as a carrier for a hydrophobic ligand. Two possible roles for such a carrier protein can be envisioned. Glick and Rothman (10) have recently shown that palmitoyl coenzyme A is a necessary cofactor for transport of protein through the Golgi stack in vitro, perhaps indicating the participation of acylated transport components in the process. A carrier protein may be required to deliver such activated long-chain fatty acids to the site of their consumption. Alternatively, Wieland et al. (26) have proposed that phospholipid transfer proteins are involved in the equilibration of phospholipids between organelles. These two scenarios for SEC14p function now provide the first experimental framework within which a direct biochemical function for the SEC14p can be tested.

The argument that SEC14p and $SEC14p_{KL}$ exhibit a functional identity is based upon our demonstration of the interchangeability of $SEC14p_{KL}$ for SEC14p in *S. cerevisiae*. This argument predicts that *K. lactis* $sec14_{KL}$ mutants will exhibit Golgi secretory defects. Given the high primary sequence homology observed between SEC14p and $SEC14p_{KL}$ (Fig. 5), it will now become possible to construct mutant $sec14_{KL}$ alleles that are directly analogous to known *sec14*(Ts) mutations. Analysis of the secretory behavior of the corresponding *K. lactis* mutants should provide an additional test of the notion that the role of SEC14p in essential Golgi secretory functions is conserved.

ACKNOWLEDGMENTS

We thank Stephen Johnston and Jon Salmeron for the *K. lactis* genomic library, Tom Stevens and Dan Klionsky for CPY and PrA antisera, and Robert Dickson and Tim Stearns for helpful discussions. Special thanks are also extended to Kathy Beal for expert preparation of the manuscript.

These studies were supported by a grant from the National Science Foundation (DCB-8620076) to V.A.B.

LITERATURE CITED

1. **Bankaitis, V. A., D. E. Malehorn, S. D. Emr, and R. Greene.** 1989. The *Saccharomyces cerevisiae SEC14* gene encodes a cytosolic factor that is required for transport of secretory proteins from the yeast Golgi complex. J. Cell Biol. **108:** 1271–1281.
2. **Boecke, J. D., F. LaCroute, and G. R. Fink.** 1984. A positive selection for mutants lacking orotidine-5′-phosphate decarboxylase activity in yeast: 5′-fluoro-orotic acid resistance. Mol. Gen. Genet. **197:**345–346.
3. **Botstein, D., S. C. Falco, S. Stewart, M. Brennan, S. Scherer, D. I. Stinchcomb, K. Struhl, and R. Davis.** 1979. Sterile host yeast (SHY): a eukaryotic system of biological containment for recombinant DNA experiments. Gene **8:**17–24.
4. **Cover, W. H., J. P. Ryan, P. J. Bassford, Jr., K. A. Walsh, J. Bollinger, and L. L. Randall.** 1987. Suppression of a signal sequence mutation by an amino acid substitution in the mature portion of the maltose-binding protein. J. Bacteriol. **169:**1794–1800.
5. **Crabb, J. W., S. Goldflam, S. E. Harris, and J. C. Saari.** 1988. Cloning of the cDNAs encoding the cellular retinaldehyde-binding protein from bovine and human retina and comparison of the protein structures. J. Biol. Chem. **263:**18688–18692.
6. **Deschler, J. O., G. P. Larson, and J. J. Rossi.** 1989. *Kluyveromyces lactis* maintains *Saccharomyces cerevisiae* intron-encoded splicing signals. Mol. Cell. Biol. **9:**2208–2213.
7. **Dickson, R. C., and M. I. Riley.** 1989. The lactose-galactose regulon of *Kluyveromyces lactis*, p. 19–40. *In* P. J. Barr, A. J. Brake, and P. Valenzuela (ed.), Yeast genetic engineering. Butterworth Publishers, Stoneham, Mass.
8. **Dunphy, W. G., S. R. Pfeffer, D. O. Clary, B. W. Wattenberg, B. S. Glick, and J. E. Rothman.** 1986. Yeast and mammals utilize similar cytosolic components to drive protein transport through the Golgi complex. Proc. Natl. Acad. Sci. USA **83:** 1622–1626.
9. **Emr, S. D., A. Vassarotti, J. Garrett, B. L. Geller, M. Takeda, and M. G. Douglas.** 1986. The amino terminus of the yeast F_1-ATPase β-subunit precursor functions as a mitochondrial import signal. J. Cell Biol. **102:**523–533.
10. **Glick, B. S., and J. E. Rothman.** 1987. Possible role for fatty acyl coenzyme A in intracellular protein transport. Nature

(London) **326**:309–312.
11. **Goldstein, A., and J. O. Lampen.** 1979. β-D-Fructofuranoside fructohydrolase from yeast. Methods Enzymol. **42**:504–511.
12. **Griffiths, G., and K. Simons.** 1986. The *trans* Golgi network: sorting at the exit site of the Golgi complex. Science **234**: 438–443.
13. **Hanahan, D.** 1983. Studies on transformation of *Escherichia coli* with plasmids. J. Mol. Biol. **164**:557–580.
14. **Ito, H., Y. Fukuda, K. Murata, and A. Kimura.** 1983. Transformation of intact yeast cells treated with alkali cations. J. Bacteriol. **153**:163–168.
15. **Mead, D. A., E. Szczesna-Skorupa, and B. Kemper.** 1986. Single-stranded DNA "blue" T7 promoter plasmids: a versatile tandem promoter system for cloning and protein engineering. Protein Eng. **1**:67–74.
16. **Novick, P., C. Field, and R. Schekman.** 1980. Identification of 23 complementation groups required for post-translational events in the yeast secretory pathway. Cell **21**:205–215.
17. **Rothstein, R. J.** 1983. One-step gene disruption in yeast. Methods Enzymol. **101**:202–211.
18. **Russell, P., and P. Nurse.** 1986. *Schizosaccharomyces pombe* and *Saccharomyces cerevisiae*: a look at yeast divided. Cell **45**:781–782.
19. **Salmeron, J. M., Jr., and S. A. Johnston.** 1986. Analysis of the *Kluyveromyces lactis* positive regulatory gene LAC9 reveals functional homology to, but sequence divergence from, the *Saccharomyces cerevisiae GAL4* gene. Nucleic Acids Res. **14**:7767–7781.
20. **Sanger, F., S. Nicklen, and A. R. Coulson.** 1977. DNA sequencing with chain-terminating inhibitors. Proc. Natl. Acad. Sci. USA **74**:5463–5467.
21. **Schauer, I., S. Emr, C. Gross, and R. Schekman.** 1985. Invertase signal and mature sequence substitutions that delay intercompartmental transport of active enzyme. J. Cell Biol. **100**:1664–1675.
22. **Sherman, F., G. R. Fink, and J. B. Hicks.** 1983. Methods in yeast genetics. Cold Spring Harbor Laboratory, Cold Spring Harbor, New York.
23. **Silhavy, T. J., M. L. Berman, and L. W. Enquist.** 1984. Experiments with gene fusions. Cold Spring Harbor Laboratory, Cold Spring Harbor, New York.
24. **Sreekrishna, K., and R. C. Dickson.** 1985. Construction of strains of *Saccharomyces cerevisiae* that grow on lactose. Proc. Natl. Acad. Sci. USA **82**:7909–7913.
25. **Stevens, T., B. Esmon, and R. Schekman.** 1982. Early stages in the yeast secretory pathway are required for transport of carboxypeptidase Y to the vacuole. Cell **30**:439–448.
26. **Wieland, F. T., M. L. Gleason, T. A. Serafini, and J. E. Rothman.** 1987. The rate of bulk-flow from the endoplasmic reticulum to the cell surface. Cell **50**:289–300.
27. **Woolford, C. A., L. B. Daniels, F. J. Park, E. W. Jones, J. N. Van Arsdell, and M. A. Innis.** 1986. The *PEP4* gene encodes an aspartyl protease implicated in the posttranslational regulation of *Saccharomyces cerevisiae* vacuolar hydrolases. Mol. Cell. Biol. **6**:2500–2510.